Annu. Rev. Earth Planet. Sci. 2004. 32:403–33
doi: 10.1146/annurev.earth.32.101802.120252

First published online as a Review in Advance on February 18, 2004

INFLUENCE OF THE MENDOCINO TRIPLE JUNCTION ON THE TECTONICS OF COASTAL CALIFORNIA

Kevin P. Furlong
Geodynamics Research Group, Department of Geosciences, Pennsylvania State University, University Park, Pennsylvania 16801; email: kevin@geodyn.psu.edu

Susan Y. Schwartz
Earth Sciences Department and IGPP, University of California, Santa Cruz, California 95064; email: sschwartz@es.ucsc.edu

Key Words lithospheric structure, San Andreas, Gorda plate

■ **Abstract** The migration of the Mendocino triple junction through central and northern California over the past 25–30 million years has led to a profound change in plate interactions along coastal California. The tectonic consequences of the abrupt change from subduction plate interactions north of the triple junction to the development of the San Andreas transform system south of the triple junction can be seen in the geologic record and geophysical observations. The primary driver of this tectonism is a coupling among the subducting Juan de Fuca (Gorda), North American, and Pacific plates that migrates with the triple junction. This coupling leads to ephemeral thickening of the overlying North American crust, associated uplift and subsequent subsidence, and a distinctive sequence of fault development and volcanism.

INTRODUCTION

Few places on the globe are as tectonically active as the Coast Ranges of northern California. In this region, complex interactions among the Pacific, North American, and Gorda plates (southernmost remnant of the ancient Farallon plate) at the Mendocino triple junction (MTJ) produce unusually fast rates of surface uplift and crustal deformation, abundant seismic activity, high heat flow, and the eruption of volcanic rocks at Earth's surface (Figure 1). Although the locus of this activity is centered on the current triple junction position, the effects of its northward migration are strongly imprinted in the geology of coastal California from the present latitude of Los Angeles through today's location of the triple junction. The MTJ was formed approximately 30 Ma when part of the Pacific-Farallon ridge system first contacted the North American-Farallon trench (Atwater 1970). Geometric consequences of the motions of the three plates resulted in the

formation of two triple junctions, a transform-transform-trench (FFT) triple junction, the MTJ, which migrated to the northwest, and a ridge-transform-trench (RFT) triple junction, the Rivera triple junction (RTJ), which moved to the southeast. Between the two triple junctions, subduction was replaced by transform motion along the growing San Andreas fault (SAF). This review explores the effects that this profound change in plate tectonic processes had on the North American lithosphere.

Assuming rigid plates, northward migration of the MTJ requires that a void or slab window develop as the Gorda plate moves northwest beneath the North American plate, extending the San Andreas fault system (SAFS). Dickinson & Snyder (1979), Lachenbruch & Sass (1980), and Zandt & Furlong (1982) recognized early that the structural and thermal state of the North American lithosphere in this region was consistent with emplacement of asthenospheric mantle material into the slab window. The geophysical signatures of heat flow, crustal and upper mantle seismic velocity, crustal deformation, seismicity patterns, and fault structure are all compatible with the slab window model. The most recent geophysical observations and geodynamical modeling have allowed Furlong & Govers (1999) to redefine the role of the North American lithosphere as involving active participation rather than passive response in the emplacement and evolution of the asthenospheric-mantle filling of the slab window. The principal conceptual modification to previous slab window models is that the effects of cooling and accreting the emplaced asthenosphere at both the southern edge of the Gorda plate and the base of the North American plate are considered. This cooled asthenosphere now part of both the Gorda and North American plates remains in mechanical continuity with the result that migration of the Gorda plate drives deformation in the overlying North American crust through viscous coupling within and along the margins of the slab window. This produces first a thickening of crust in advance of the triple junction and then thinning of the thickened crust after triple junction passage. The implications of this changing model for MTJ tectonics extend far beyond simply explaining the pattern of crustal structure near the MTJ. The ephemeral thickening and concomitant metamorphism of crustal material newly accreted to the continental convergent margin may be an important new process in the production of continental crust of accretionary margins.

The generation of continental crust has been and still remains a fundamental issue in the Earth Sciences. Several proposed mechanisms for crustal generation have been long lived in the scientific literature. These include (*a*) the conventional andesite model (McLennan & Taylor 1982), where continents grow through accretion of andesitic arcs to existing continental margins; (*b*) oceanic plateau accretion and subsequent magmatism (Stein & Goldstein 1996); and (*c*) plume-driven magmatic underplating of existing crust. Although andesite, believed to be closest to the bulk composition of continental crust, is often an abundant rock type at island arcs, the gross composition of most arcs is too mafic compared with typical continental crust (e.g., Holbrook et al. 1999). Therefore, like mechanism (*b*), if island arcs form a significant component of continental crust, the composition of the arc

crust must be substantially modified to become more felsic. Both magmatism and delamination of mafic lower crust during or after accretion have been proposed as mechanisms of silica enrichment. More recently, lateral growth of continental crust through subduction accretion (Johnson et al. 1991, Kimura et al. 1993, Barr et al. 1999, Sengor & Natalin 1996) has gained prominence. This method achieves crustal growth through the accretion of supracrustal rocks at convergent margins, and therefore adds siliceous components to existing continental crust. The difficulty with this crustal generation model is that the largely felsic crust needs to be made more mafic to be consistent with observations of an overall andesitic composition for bulk continental crust. Typical lower continental crust appears to consist of granulite or other high-grade metamorphic facies rocks (Rudnick & Fountain 1995). The additional heat and potential basaltic underplating produced by slab window asthenosphere, together with the ephemeral crustal thickening and thinning resulting from viscous coupling of asthenosphere and crust, may be sufficient to convert a subduction accretion complex, such as the Franciscan Terrane into more typical continental crust.

This review begins with a tutorial on rigid plate tectonics to demonstrate that the MTJ migrates at the velocity of the Pacific plate relative to North America and that a slab window develops in the wake of this migration. It then reviews the geologic setting of the MTJ and the manifestations of the slab window in the geophysical and geologic observations of heat flow, Cenozoic volcanism, lithospheric structure, crustal deformation, and seismicity. We more fully develop the dynamic slab window model (Furlong & Govers 1999), here termed the Mendocino crustal conveyor (MCC) model, and show how it reconciles some of the inconsistencies left by only considering a process with passive asthenospheric upwelling into the slab window.

KINEMATICS OF THE MENDOCINO TRIPLE JUNCTION

The MTJ serves as the archetype FFT triple junction. In spite of the almost universal recognition of its basic kinematic behavior, there is still significant confusion and/or uncertainty as to the implications of the surface plate motions for the three-dimensional (3-D) plate boundary geometry and evolution. Here we undertake a brief review of the kinematic evolution of the MTJ with a focus on how surficial plate motions generate the 3-D plate boundary structure that we image geophysically.

Some of the confusion about plate boundary development in this area may be a consequence of a few misunderstandings common in introductory textbooks. It is often stated or at least implicitly assumed that the SAFS developed as a consequence of ridge subduction—the implication is that along the entire margin of California, segments of the Farallon-Pacific ridge were subducted. Although ridge subduction played an important role in the evolution of the southern (Rivera) triple junction, its role in the evolution of the MTJ was restricted to the initial stages

of triple junction formation. Further, the near-surface manifestation of the plate boundary in the various components of the SAFS is complex and has evolved as the plate boundary has matured. How this near-surface complexity maps into lithospheric scale structures is not clear, but it appears that there is not a one-to-one correspondence. Finally, it is important to differentiate between processes that occurred during the initial formation of the MTJ, when a mid-ocean ridge and newly generated oceanic lithosphere were involved in triple junction deformation, and the present plate boundary geometries and kinematics at the triple junction.

In Figure 2, a schematic representation of the initial development of the MTJ (and paired RTJ) is shown. Prior to the interaction of the Pacific-Farallon ridge with the North American margin, subduction of the Farallon plate occurred along the entire margin. Two characteristics of the Pacific-Farallon margin were important in the spawning of the MTJ and its structure. The ridge separating the Pacific and Farallon plates had an approximate north-northeast trend, resulting in very oblique convergence between the North American margin and the ridge as it approached the trench. Second, the ridge-transform system that separated the Pacific and Farallon plates was characterized by large offset transforms separating the ridge segments. Because of the obliquity of Farallon–North American subduction and the orientation of the ridge, Pacific–North American relative plate motion was subparallel to the North American margin. As a result, once Pacific plate material came into contact with the North American margin, convergence across that segment of the boundary was lost, and the San Andreas transform was born. Although the ridge continued to generate lithosphere, only that lithosphere produced on the southern (Farallon) flank of the ridge was subducted. Material produced on the Pacific flank will move along the North American plate margin.

The consequence of no subduction occurring north of the ridge intersection, as shown in Figure 2*b*, is the cause of the generation of the slab window. Material produced on the Farallon side of the ridge follows Farallon–North American motion (north-northeast; Figure 2*a*), whereas lithosphere generated on the Pacific side moves along the margin according to Pacific–North American motions. The net result is the development of a slab window or slab gap along the margin (Dickinson & Snyder 1979, Zandt & Furlong 1982, Atwater & Stock 1998). This occurred because of the relative motions involved and the existence of the long offset Mendocino transform fault. Essentially, the SAF lengthens as the Mendocino fault shortens. The corner of the Pacific plate at the intersection of the Mendocino fault and SAF is a long-lived feature, as it is bounded by two transform (conservative) boundaries. Thus, it represents the oldest part of the San Andreas plate boundary. In contrast, the North American lithosphere just to the east of that corner has recently been transferred from being part of the subduction boundary to lying adjacent to the transform, so it is the youngest part of the plate boundary. This contrast in lithospheric boundary maturity plays an important role in the evolution of the triple junction and the SAFS.

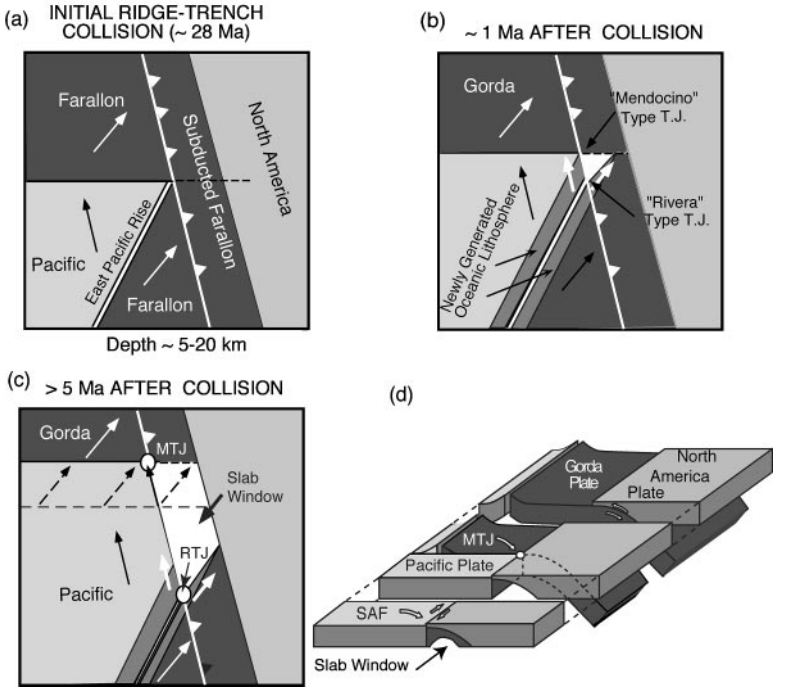

Figure 2 Schematic view of the plate tectonic evolution that led to the formation of the MTJ and the resulting slab window. (*a*) Initial plate configuration just prior to triple junction formation. Arrows indicate directions of movements of Pacific (PAC) and Farallon (FAR) plates with respect to North America (NOAM). (*b*) Plate configuration immediately after the formation of the MTJ and the associated RTJ. Short white arrows indicate motion of newly formed oceanic lithosphere with respect to NOAM. (*c*) Plate configuration after the triple junctions have stabilized and separated. Dashed line and dashed arrows indicate the path of the Mendocino Fracture Zone through time and the development of a sharp northern edge to the slab window. Solid arrow along plate boundary indicates MTJ motion. (*d*) Three-dimensional sketch of the development of the slab window in the vicinity of the MTJ. The initial shape of the slab window should mimic the geometry of the previously subducted Gorda slab.

Stepping forward in time, the role of a spreading center in the kinematics of the MTJ became insignificant. The spreading center remained a defining component of the southern RTJ. As the two triple junctions migrated apart, the thermal and structural impact of the spreading center no longer affected the MTJ (Figure 2*c*). At that time, plate velocities required that the MTJ migrate at the rate and direction of Pacific–North American relative motion. As a result, the northern extent of the San Andreas lengthened at that rate. What matters more for the evolution of the North American lithosphere is the behavior of the Farallon plate (whose remnant is

termed the Juan de Fuca plate, with the term Gorda plate used for the southernmost Juan de Fuca just north of the triple junction). To quantify the kinematics, we need only consider the relative behavior of the Gorda and North American plates and the geometry of the southern boundary of the Gorda plate defined by the Mendocino transform (Figure 2*c*). The Mendocino transform is oriented approximately east-west, so that combined with the northeast relative motion between the Gorda plate and North America, the southern margin of the Gorda plate migrates to the north (again at the Pacific–North American rate, as the Mendocino transform also defines the northern edge of the Pacific plate).

Although this is well understood and universally recognized for the surface extent of the Gorda plate, what happens to the southern edge of the Gorda plate in the subsurface beneath the North American margin is a point of some discussion in the literature. Our position is that subject to minor modifications resulting from some internal deformation to the Gorda plate and small changes in relative motion over the past 15 million years, the southern edge of the subducted slab migrates in concert with the triple junction, forming an abrupt end to the subduction beneath northern California (Figure 2*c*). Others (Page & Brocher 1993, Bohanan & Parsons 1995, ten Brink et al. 1999) have argued that perhaps the slab is left behind as the triple junction migrates, negating the need to develop a slab window. We do not think this is a sustainable interpretation, as it would require slicing off entire sections of the slab in concert with MTJ migration. The oblique nature of Gorda–North American motion would produce a notch type pattern to the southern edge of the subducted slab, and a period of several million years would be needed before the slab at its southern edge again extended to the east. This is incompatible with the occurrence of volcanism in the southern Cascadia arc and with tomographic images of the upper mantle (Benz et al. 1992). North of the triple junction, the subducted Gorda slab appears to extend continuously into the upper mantle with a well-defined southern edge (Figure 1), consistent with the kinematic model. The Gorda plate in its subducted extent does undergo internal deformation, and that modifies slightly the orientation of the slab and its southern edge. The result of this is a slight southeasterly trend to the southern edge as observed in patterns of seismicity and tomographic images (Figures 5 and 7).

The net result of this plate boundary evolution is the development of a slab window that is limited on the north by the southern edge of the subducted Gorda slab and on the west by the eastern edge of the translating Pacific lithosphere. The eastern extent of the slab window is defined by the geometry of the base of the North American plate. North of the MTJ, the base of North America mirrors the geometry of the subducted slab. Thus where that slab has been removed, there is a taper to the base of the lithosphere (Figure 2*d*). The eastern margin of the slab window is therefore dependent on the depth, with the slab window broadening as one goes deeper. In terms of most of the consequences discussed here, the effects are dominantly shallower than 100 km depth. Thus, the slab window forms a swath along coastal California defined on the west by the SAF and along the east by the eastern side of the Coast Ranges.

GEOLOGIC SETTING OF THE MENDOCINO TRIPLE JUNCTION

Figure 3 shows the geologic and tectonic setting of northern coastal California. Basement rocks in the vicinity of the MTJ primarily consist of the Franciscan Complex, a Mesozoic- to Cenozoic-aged, uplifted, and exhumed subduction zone accretionary wedge. The Franciscan Complex primarily consists of sandstones, shales, cherts, metagraywackes, melanges, mafic volcanics, and some high-grade metamorphic rocks in blueschist and eclogite facies that document subduction and rapid uplift. The Franciscan Complex is comprised of individual beds that are often discontinuous with large bodies of rocks of differing lithology frequently in contact. The Franciscan Complex has been divided into three parallel belts based on differences in lithology, structural fabric, and the degree of metamorphism (Blake et al. 1985). In general, rock age and metamorphic grade increase from west to east, transversing the Coastal, Central, and Eastern Belts (Figure 3). Rocks of the Coastal Belt are made up of late Cretaceous to early Cenozoic sedimentary rocks that are metamorphosed to at most zeolite facies. Metamorphic grade progresses to blueschist/greenschist facies in the Eastern Belt, following the expected pattern of high-pressure, lower-temperature metamorphism common to subduction zone accretionary prisms (Ernst 1970). Cenozoic volcanic rocks outcrop as isolated volcanic centers that decrease in age from south to north (southernmost volcanics shown in Figure 3 are the Sonoma volcanics ∼3–7 Ma and northern volcanics are the Clear Lake volcanics ∼2–0.1 Ma). North of the MTJ, the crustal section above the subducted Gorda plate near the coast appears to be composed entirely of Franciscan Complex material.

MANIFESTATIONS OF TRIPLE JUNCTION MIGRATION

Following Atwater's (1970) and Dickinson & Snyder's (1979) seminal work on the kinematics of the MTJ, numerous studies modeling gravity (Jachens & Griscom 1983), heat flow (Lachenbruch & Sass 1980, Zandt & Furlong 1982, Furlong 1984), teleseismic P wave delay (Zandt 1981, Zandt & Furlong 1982), and geochemical data (Johnson & O'Neil 1984, Fox et al. 1985) from the California Coast Ranges established details of the geometry of plate interactions. In particular, these studies demonstrated the role of the migrating triple junction and the profound influence that mantle upwelling into the space vacated by the northward moving Gorda plate has had on the tectonics of coastal California. Hundreds of papers have been published over the past 25 years that incorporate the slab window concept into their analysis. It is not an overstatement to say that the MTJ slab window model has dramatically altered the way in which we view the evolution of coastal California and the northern SAFS. Rather than review this huge body of work in its totality, this paper focuses on the more recent observational and modeling efforts. These recent studies provide improved constraints on the kinematics and dynamics of

the transition from convergent to transform motion in the wake of the migrating triple junction and allow us to introduce a fundamental revision for MTJ tectonics where there is much more active coupling between the upwelling asthenosphere and the surrounding lithosphere than previously acknowledged.

Heat Flow and Thermal Regime

Observations of heat flow through the northern Coast Ranges have played a critical role in the development of models for the tectonic consequences of MTJ migration. The heat flow data set that straddles the transition from subduction to transform (Lachenbruch & Sass 1980) demonstrated that the elevated heat flow seen through much of the Coast Ranges did not display the localized anomaly predicted to result from shear heating along the SAFS. The heat flow anomaly has several diagnostic characteristics (Figure 4). As expected in a subduction environment, heat flow is low overlying the subducting Gorda slab, with values in the 40–50 mW/m^2 range. Moving south of the triple junction, heat flow through the Coast Ranges rises to values of approximately 90 mW/m^2. Key to linking the rise in heat flow to MTJ and slab window processes is the distance south of the triple junction (and equivalently time since MTJ passage) over which the heat flow increases. Over a

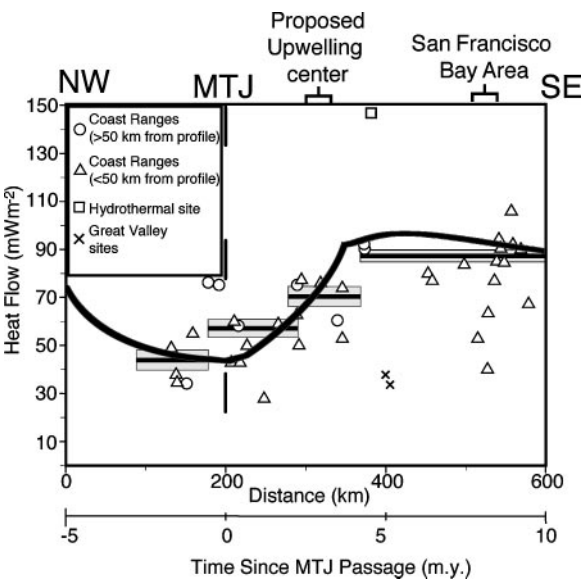

Figure 4 Heat flow in northern California along a swath in the Coast Ranges. Data are from Lachenbruch & Sass (1980). Solid line shows fit of time-dependent thermal modeling, including the effects of MCC-driven crustal thickening/thinning (Guzofski & Furlong 2002). Horizontal bars and surrounding boxes indicate average values with standard deviations.

distance of approximately 200 km (∼4–5 million years) the observed surface heat flow approximately doubles. This is consistent with a source for the anomalous heat at depths of 15–25 km (Lachenbruch & Sass 1980, Zandt & Furlong 1982, Furlong 1984, Furlong et al. 1989). The heat flow maintains high values through the northern Coast Ranges, implying additional sources of heat beyond simple secular cooling of material in the slab window mantle. Candidate sources for this heat include latent heat of crystallization from underplated mafic magmas derived from pressure relief melting of the upwelling asthenosphere (Liu & Furlong 1992) and perhaps small-scale convective motions in the emplaced slab (Liu & Zandt 1996).

This pattern of heat flow has been used to develop models of Coast Range thermal structure, which have been compared to the depth distribution of seismicity through the Coast Ranges (Miller & Furlong 1988, Castillo & Ellsworth 1993, Goes et al. 1997). Because both the spatial distribution and the amplitude of the Coast Range thermal anomaly are explainable by slab window thermal processes, the need to invoke frictional heating along the SAFS as a cause of the high heat flow is reduced, providing additional support for models of a relatively weak SAFS through the Coast Ranges. Key to these models of thermal evolution was the rise of the heat flow anomaly time (∼200 km or ∼4–5 million years), implying a thin crustal lid (15–25 km) above the emplaced slab window mantle.

Petrogenesis of Cenozoic Volcanics

The emplacement of hot asthenospheric mantle to shallow levels beneath the western margin of North America could be expected to generate melt and possibly magmatism. Consistent with this expectation is a sequence of volcanic centers that have erupted in the wake of the triple junction within the Coast Ranges (Johnson & O'Neil 1984, Dickinson 1997). The youngest of these volcanic centers is the Clear Lake volcanics (Figure 3), which have erupted since ∼2 Ma. In addition to surface volcanics, the magmatism associated with MTJ migration could lead to significant plutonic additions to the overlying North American crust (Liu & Furlong 1992).

Whether the mantle that fills the slab window following slab migration is derived from subslab mantle from below or supraslab (mantle wedge) mantle to the east will affect its chemistry, thermal conditions, and physical properties. Geochemical analyses of basalts and basaltic andesites from the Coast Range volcanic centers (Whitlock 2002, Whitlock et al. 2001) indicate a pattern in trace elements that closely matches the pattern observed in Cascade arc volcanics. As is typical of mantle wedge–derived melts, there is an enrichment in the large-ion lithophile elements (LILE), such as Ba and K, as compared to chondritic mantle, and a depletion in the high-field-strength elements (HFSE), such as Nb, Ta, and Ti. This is in contrast to the chemistry of mid-ocean ridge–type basalts, which have a distinctively different pattern of depletions and enrichments. The implication of this chemistry for the genesis of the Coast Range volcanics is that the asthenospheric

mantle that fills the slab window is likely derived from the mantle wedge to the east. In this way, the northern Coast Range volcanic centers tap the same primary source material as the arc volcanics of the Cascade volcanoes, providing an alternative means of sampling the mantle wedge. This also implies that the mantle emplaced into the slab window may be quite hydrous, of lower viscosity, and lower in temperature than it would be if it were derived from the subslab mantle.

There is a time lag between passage of the MTJ and the eruption of the Coast Range volcanics of approximately 3 million years (Dickinson 1997). Initially, this was thought to reflect the time necessary for the magmatic system to become established (e.g., Liu & Furlong 1992), but it may simply reflect the spatial pattern of mantle inflow into the slab window.

Lithospheric Structure

With the passage of the MTJ there is a profound change in the plate boundary structure through coastal California. North of the triple junction, the subducting Gorda slab underlies a tapered western edge to North America that thickens to the east. South of the triple junction, this thin edge of North America lies above the emplaced slab window mantle. Constraints on lithospheric structure near the MTJ come principally from seismic refraction-reflection profiles carried out during the 1993–1994 Mendocino Triple Junction seismic experiment (MTJSE) (e.g., Trehu et al. 1995, Beaudoin et al. 1996), 3-D P-wave velocity images from tomographic inversion of local earthquake arrival times (Verdonck & Zandt 1994, Villasenor et al. 1998), and teleseismic receiver function analysis (Hall et al. 2001). Each of these different methods is best at resolving particular attributes of lithospheric structure. When combined in one region, they can provide strong constraints on the architecture of the lithosphere. Seismic refraction/reflection imaging allows abrupt changes in seismic velocities and thickness of crustal layers to be determined, primarily along two-dimensional (2-D) cross-sections. Seismic refraction studies usually define the gross characteristics and penetrate deeper into Earth, whereas reflection studies fill in finer details of the shallower structure. Inversion of earthquake arrival times for seismic structure (tomography) can extend models into the third dimension and resolve velocity structure to great depth, but does not successfully image abrupt horizontal velocity changes. Receiver function analysis provides point determinations of horizontal stratification beneath a seismic station. Although it provides structural information over a very limited areal extent, receiver function analysis is the preferred technique for determining the depths to and velocity and density contrasts across sharp horizontal discontinuities, such as the Moho. Because most refraction/reflection and seismic tomography studies use P waves alone, receiver function analysis often provides the only constraint on the shear wave velocity structure of the lithosphere.

The onshore portion of the MTJSE consisted of an approximate 250 km north-south refraction-reflection profile from north of Eureka to Clear Lake, California

(Line 9 on Figure 1 and Figure 5), that crossed the transition from convergent to transform motion. Together with two shorter (∼200 km) east-west profiles, one north and one south of the MTJ (Lines 6 and 1 on Figure 1), variations in the lithospheric structure of North America have been inferred to below 20 km depth. The primary results of the MTJSE are images of the P-wave velocity along the three profiles (Figure 5). North of the MTJ, the structure consists of ∼10–14 km of low P-wave velocity ($v_p \leq 5.5$ km/s) material overlying higher velocities ($v_p = 6.2$–7.0 km/s). This structure is consistent with the data from a 140-km-long refraction-reflection, coast-parallel profile previously recorded by Stanford University and the U.S. Geological Survey (Beaudoin et al. 1994). Beaudoin et al. (1994) attributed the low velocities to the Franciscan Complex, which outcrops at the surface in this region (Figure 3). The higher velocities below the Franciscan were interpreted as Gorda plate lithosphere, with two prominent reflections occurring at the top and bottom of the Gorda crust. Three-dimensional images of crustal structure immediately north of the MTJ, derived from seismic tomography, confirm a depth of approximately 15 km to the top of the Gorda Plate near the shoreline (Verdonk & Zandt 1994). Prior to modification by triple junction passage, the North American crust appears to be both uniform and simple, created by the process of accretion of subduction zone complex materials to the margin of North America.

However, images of crustal structure south of the triple junction indicate that the North American crust is significantly modified by triple junction passage. Line 1 and portions of line 9 south of the MTJ indicate the existence of a layer with seismic velocities between 6 and 7 km/s that varies in thickness between 8 and 25 km (Figure 5). This layer, sandwiched between low-velocity Franciscan rocks and much higher velocities ($v_p > 7.0$) indicative of mantle, is interpreted as mafic lower crustal material (Beaudoin et al. 1996). A similar mafic lower crustal layer has been observed above the Moho by every other seismic reflection/refraction experiment in the Coast Ranges, and its origin has been the subject of considerable conjecture (Hole et al. 1998). Although it has been suggested that this mafic layer reflects either a slab of Pacific oceanic lithosphere filling the gap left by the northward moving Gorda slab (Page & Brocher 1993) or fragments of the Gorda plate broken off and stranded beneath North America (Bohanan & Parsons 1995), vertical offsets of this layer below the surface expression of several strike-slip faults of the SAFS are inconsistent with these interpretations (Henstock et al. 1997, Hole et al. 2000). Instead, magmatic underplating in the slab window is a preferred explanation. Very strong seismic reflectivity at the top and continuing throughout the mafic layer along seismic line 9, which is interpreted as resulting from discrete zones of partial melt segregated from asthenospheric upwelling into the slab window (Levander et al. 1998), provides strong support for this model.

In addition, the total crustal package thickens dramatically along line 9, south of the MTJ, reaching an apparent maximum of at least 35 km north of shotpoint 906 and thinning to less than 20 km south of shotpoint 904 (Figure 5). This crustal

thickening is visible in the 3-D seismic crustal tomography images (Verdonk & Zandt 1994, Villasenor et al. 1998) as a welt of low-velocity material extending to 35–40 km depth in the vicinity of seismic station CVLO (Figures 1 and 5). Somehow, in the 2 million years since passage of the MTJ, 10–14-km-thick accretionary complex material must have been transformed into more typical crust being first substantially thickened and then thinned in the process.

The strong velocity contrast between the silicic Franciscan rocks of the upper crust and the underlying lower crustal mafic layer produce a distinct seismic reflection identifiable in the travel-time curves from the MTJSE (Hole et al. 1998). The strong P-wave velocity contrast at this layer is also well imaged by teleseismic receiver functions. This technique, which isolates the P-S response of the layered subsurface structure beneath a particular station, provides some constraints on the S-wave velocity and density contrasts across strong boundaries, and thus improves the assignment of rock compositions to specific velocity/density layers. Pennsylvania State University and University of California, Santa Cruz, deployed two broadband seismic stations (CVLO and FREY) in the region of North American lithosphere most recently modified by passage of the MTJ (Figure 1 and 5). Two existing broadband stations, HOPS (Berkeley Digital Seismic Network) and KCPB (U.S. Geological Survey), have been operating in this region since 1995 and 2001, respectively. Receiver function analysis of teleseismic events recorded at these stations has been performed and provides detailed information on fundamental velocity boundaries in the crust beneath the stations.

Stacked receiver functions from tens of events at varying azimuths, along with synthetic receiver functions for our preferred crustal models, are shown for all four stations in Figure 6. P to S conversions and reflections from strong crustal boundaries are identified on the receiver functions (bottom right of Figure 6), and their raypaths are indicated on the preferred velocity model for station CVLO. Here two strong interfaces exist at 13 and 26 km, with raypaths and nomenclature for P to S conversions and reflections indicated for the shallower interface only. These same phases, from interfaces at slightly different depths, are identified on the stacked receiver functions from the remaining stations. The velocity structures obtained from receiver function modeling show many of the features revealed in the seismic tomography and reflection/refraction profiling. The depths of the primary interfaces observed in the receiver function analyses are shown in the tomography cross sections in Figure 5 at the approximate location of each station. A strong velocity and density contrast between low-velocity upper crust ($v_p \leq$ 5.5 km/s) and higher-velocity lower crust or mantle is apparent beneath all stations (Figure 6). The depth of this boundary shallows slightly from approximately 18 km beneath the southernmost station (HOPS) to 13 km beneath the northernmost station (CVLO). Whereas the low-velocity crust thins from south to north, the entire crustal thickness increases from 18–26 km to 26–35 km from south to north, in agreement with results of both the local earthquake tomography (Villasenor 1998) and the MTJSE (Figures 5 and 6; Beaudoin et al. 1996, 1998). The large range in

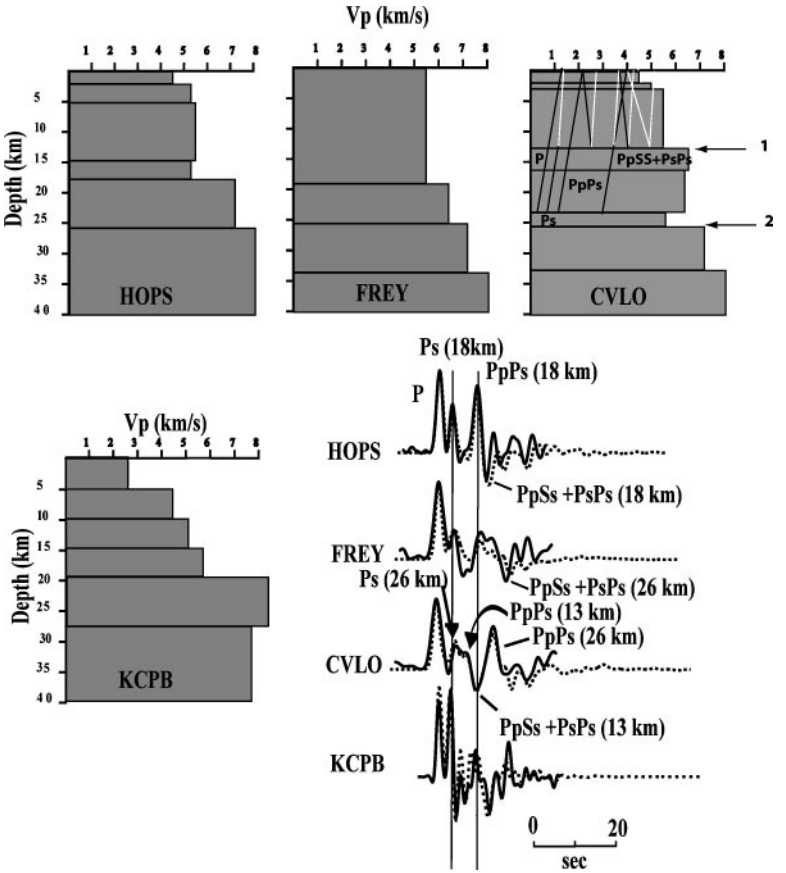

Figure 6 Stacked observed (*solid lines*) and synthetic (*dashed lines*) receiver functions with P to S conversions and reflections from strong crustal interfaces marked (*bottom right*). Preferred crustal P-wave velocity models are shown for all the stations of Figure 1 with the raypaths of prominent P (*black*) to S (*white*) conversions and reflections from a 13 km interface indicated for station CVLO. Numbered arrows on the CVLO crustal model indicate the location of two dominant interfaces that generate obvious arrivals in the receiver function stack for this station. We interpret these to represent intracrustal layering.

crustal thickness assigned for the stations reflects two possible interpretations for the Moho. If it occurs at the greater depth, the $v_p = 7.22$ km/s layer just above it represents magmatic underplating of mafic material derived from upwelling of the asthenosphere that fills the slab window. If a shallower Moho is preferred, the mafic layer would represent the hot asthenospheric material occupying the slab window.

Crustal structure revealed through receiver function analysis at the southernmost station HOPS (Figure 6) is relatively simple, and our preferred rock-type assignments based on modeling of constant P- and S-wave velocity and density layers are ∼18 km of moderately metamorphosed Franciscan crust above ∼8 km of underplated mafic magmatic rock overlying the mantle. Because no significant conversions or reflections are observed from a boundary below the mafic layer, we have little resolution on the thickness of this layer or on the velocities and density of the lowest layer (interpreted as mantle). We assign a thickness for the mafic layer and velocities for the upper mantle that are consistent with results of the MTJSE (Beaudoin et al. 1996) and other reflection/refraction experiments in the Coast Ranges (Hole et al. 1998). The rock-type assignments for the crust beneath our northernmost station, CVLO, are ∼13 km of unaltered Franciscan crust overlying ∼11 km of Franciscan metamorphosed to prehnite-pumpellyite and felsic granulite grade overlying ∼10 km of underplated mafic rock with the upper 1–2 km containing a substantial melt fraction or metamorphically derived fluids. An alternative interpretation would assign the low-velocity layer at ∼25 km depth to granulite-grade metamorphosed Franciscan with melt or fluid pockets and the high-velocity layer just below it to asthenosphere. Analysis of receiver functions from the central station FREY reveals a crustal structure similar to CVLO, our rock-type assignments are ∼19 km of unaltered Franciscan overlying ∼7 km of felsic granulite-grade metamorphosed Franciscan overlying ∼8 km of underplated mafic rock or asthenosphere. Crustal structure beneath the coastal station KCPB shows similar characteristics for the upper crust, but at ∼19 km there is a sharp jump in velocity to over 8 km/s (Figure 5*c*,*d*; Figure 6) (Hayes et al. 2003). We interpret this velocity interface to represent the top of a relict piece of Farallon plate that became attached to the Pacific when the short ridge segment that separated the Pioneer and Mendocino transforms approached the trench approximately 25 Ma. This Pioneer fragment appears to have been moving along the western margin of North America, in many ways similar to the way in which the Gorda slab is moving north.

Because the North American crust north of the MTJ is composed entirely of Franciscan Formation rocks, and the Franciscan at the surface is known to consist of a variety of rock types, including graywacke, basalts, and serpentine, its reasonable to assign the moderate velocity layers (6.4 km/s $\leq v_p \leq$ 6.6 km/s) found at depths between 13–26 km beneath CVLO and FREY to be various compositional units of the Franciscan metamorphosed to different grades. The substantial thickening of the Franciscan crust associated with passage of the MTJ would carry the Franciscan formation to appropriate depths to metamorphose it to prehnite-pumpellyite grade (Furlong & Guzofski 2000), and with increased temperatures associated with asthenospheric upwelling in the slab window, possibly to granulite grade. The crust thins to the south at HOPS, apparently by preferential thinning of the lower crust and essentially complete loss of the metamorphosed Franciscan layers present below the two northern stations.

Crustal and Lithospheric Deformation

In the vicinity of the MTJ, we expect to see dramatic differences in observed crustal deformation. North of the triple junction, convergence between the Gorda and North American plates should be manifested as crustal shortening in the direction of relative plate motion. South of the triple junction, crustal deformation should primarily reflect the interaction between the Pacific and North American plates. North of the triple junction, a dominant signal in present-day shortening, as observed by global positioning system (GPS) studies, is the interseismic strain accumulation that is released during mega-thrust earthquakes (McCaffrey et al. 2000). To the south of the triple junction, crustal strain from GPS observations indicates a 100-km-wide region over which approximately 40 mm/year of relative motion is accommodated (Freymueller et al. 1999).

In northern California the Pacific–North American plate boundary is in nearly perfect strike-slip motion with essentially no transpression. GPS observations show at most only a few millimeters per year of fault-normal shortening across the 100-km-wide zone of right lateral shear (Freymeuller et al. 1999), and plate motion models averaging over longer time intervals also indicate virtually no transpressional deformation (DeMets & Dixon 1999). Unfortunately, at present there are few GPS observations immediately south of the triple junction—the northern extent of the Freymeuller et al. (1999) study is approximately 100 km south of the MTJ—so the details of how the subduction-associated convergence is transformed into the San Andreas shear deformation remains unconstrained. Additionally, the GPS observations combine recoverable (elastic) strain that is released during major earthquakes with permanent deformation that will be recorded in the geology. In the vicinity of the triple junction, the recent occurrence of earthquakes (discussed in the next section) complicates the interpretation of crustal strain as observed geodetically (Murray et al. 1996). What is clear is that by the latitude of the GPS observations, faults of the northern SAFS, such as the Maacama fault through Ukiah and Willits, are well established (Kelsey & Carver 1988); are oriented in the Pacific–North American relative motion direction; and undergo fault creep at rates as high as 6 mm/year, similar to that observed on the Hayward Fault through the San Francisco Bay region (Simpson et al. 2001).

The lack of transpression along the plate boundary through the Coast Ranges raises the question of the mechanism of uplift in the Coast Ranges (Figure 1). The spatial correlation between the region of uplift and the slab window led to models of uplift driven dominantly by thermal processes (e.g., Zandt & Furlong 1982). Although the heating of the crust after MTJ passage and buoyancy in the slab window should lead to uplift, quite high temperatures were required to produce the magnitude of uplift in the Coast Ranges. Additionally, these models of uplift were based on assumptions of a thin and laterally constant crustal thickness throughout the Coast Ranges. It has become clear that the pattern of uplift is likely significantly more complex than obtainable with the smoothly varying effects of crustal heating. Patterns of river flow, migration of divides, and exhumation and deposition within

the Coast Ranges all argue for a laterally varying and migrating pattern of uplift in the Coast Ranges (Lock & Furlong 2002).

Seismicity

The region around the MTJ has one of the highest rates of seismicity in continental North America (Figure 7). Complex interactions among the North American, Pacific, and Juan de Fuca (Gorda) plates are responsible for this abundant seismic activity and generate earthquakes with a wide range of focal mechanisms.

MENDOCINO TRANSFORM FAULT, GORDA DEFORMATION ZONE, AND CASCADIA SUBDUCTION ZONE The majority of the seismicity near the MTJ is located offshore, diffusely distributed within the Gorda plate and concentrated along the Mendocino Transform (MT) (Figure 7). The small size and young age (hence thin lithosphere) of the Gorda plate, relative to the surrounding North American and Pacific plates, cause it to suffer severe internal deformation in response to north-south compression produced by oblique convergence with the Pacific plate (e.g., Silver 1971). The extreme level of internal deformation within the Gorda plate is not consistent with rigid plate tectonics and has resulted in this plate being more descriptively referred to as the Gorda deformation zone (GDZ) (Wilson 1989). The unusual behavior of the GDZ was first identified from severe bending of magnetic lineations apparent in the first magnetic anomaly map of the Pacific Ocean that supported the theory of plate tectonics (Mason & Raff 1961). Sinusoidal NE-SW-oriented structural trends in the GDZ that parallel magnetic lineations are first-order features of the seafloor bathymetry (Silver 1971, Dziak et al. 2001). These structures are believed to be left-lateral strike-slip faults that originated as ridge-parallel normal faults near the spreading Gorda ridge and were later rotated and reactivated in response to north-south shortening from Pacific plate impingement. A prominent northeast-oriented fault scarp that truncates a large sediment fan emanating from the mouths of the Mendocino and Eel river canyons (Dziak et al. 2001)

Figure 7 Seismicity in the vicinity of the MTJ from 1969–2003 (Northern California Earthquake Data Center) in map and cross-sectional views. Berkeley centroid moment tensor focal mechanism solutions are shown for the four events larger than $M_w = 6$. All earthquakes shown in map view are projected onto each cross-section; however, seismicity contained within each box is distinguished with a darker symbol in each cross-section. The arrows in cross-sections A-A′ (along the Maacama fault, MF) and B-B′ (along the Bartlett Springs fault, BSF) indicate the southern edge of the Gorda slab, which is located in map view by the solid black line; the dashed line extending much farther to the south is the slab termination determined by Jachens & Griscom (1983). The line on section A-A′ highlights the shallowing of the depth of seismicity along the Maacama fault between Laytonville (LAY) and Clear Lake (CL). CSZ: Cascadia subduction zone; SAF: San Andreas fault; MT: Mendocino Transform; RV: Round Valley; LP: Lake Pillsbury.

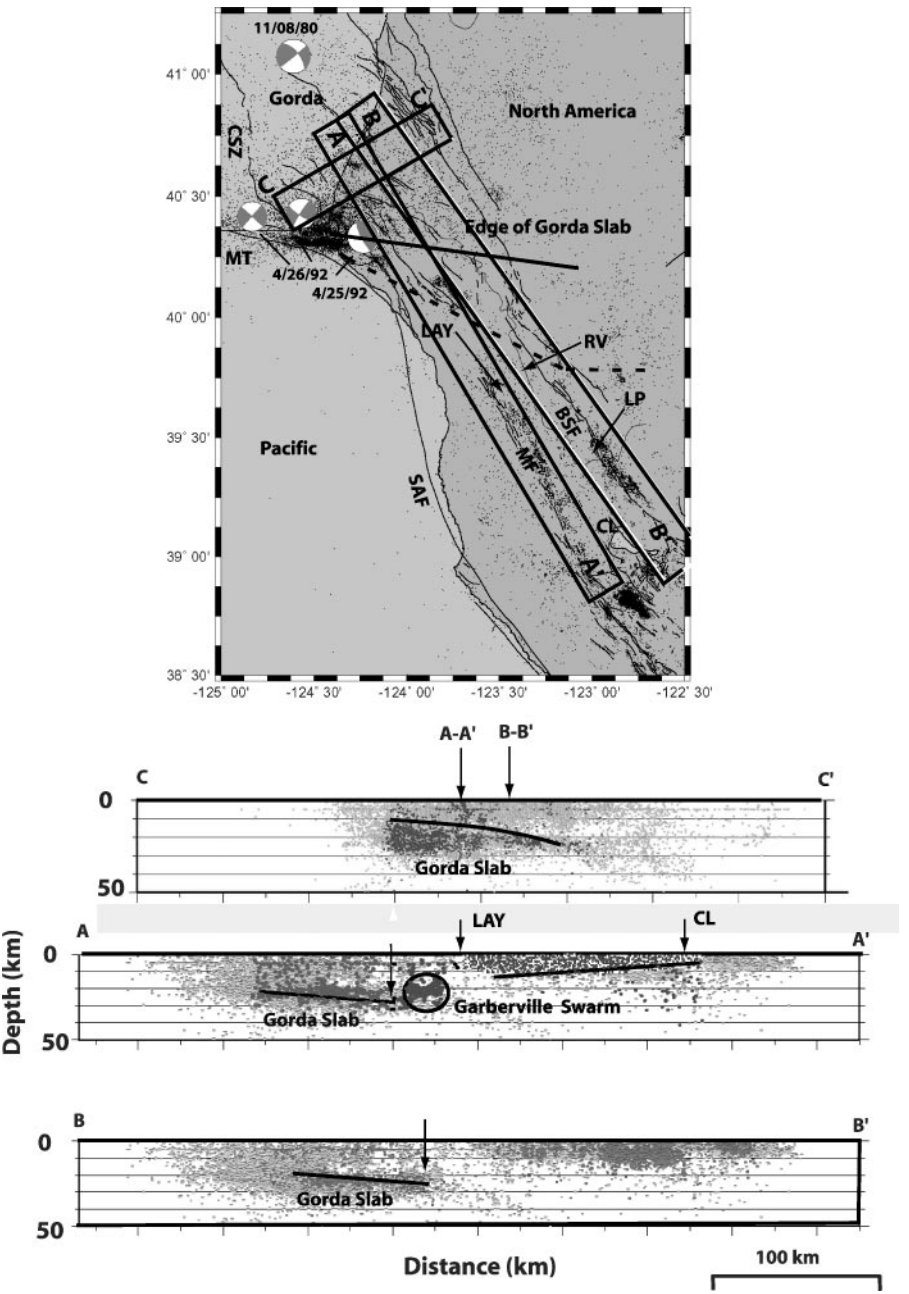

provides strong support for this interpretation. At least one large earthquake, the 1980 $M_s = 7.2$ Eureka, California earthquake (Figure 7), ruptured on a northeast oriented, left-lateral strike-slip fault (Lay et al. 1982, Eaton 1981). Two moderate-sized strike-slip earthquakes that occurred on April 26, 1992 (Figure 7), have also been interpreted as occurring on these pervasive reactivated normal fault structures (Velasco et al. 1994). Earthquakes along the Mendocino Transform indicate predominantly right-lateral motion on east-west oriented, vertically dipping planes (BDSN CMT mechanism catalog, Smith et al. 1993).

Fault orientations change abruptly within the North American crust that overlies subducted Gorda lithosphere. Here, active thrust faults in the southern portion of the Cascadia subduction margin rotate strike from north-northwest offshore (parallel to the strike of the Cascadia subduction zone) to west-northwest onshore (Figure 7) where it has been determined that they accommodate ~10 mm/year of N20°–40°E convergence (McCrory 2000). The skewed orientation of the onshore faults has been attributed to a hybrid stress field arising from the combination of Gorda–North American (~40–50 mm/year at N40°–55°E) and Pacific–North American (~22 mm/year at N35°W) plate motions (McCrory 2000). South of the MTJ the Pacific–North American plate boundary extends over a width of almost 100 km. For this broad zone to connect with the trench and Mendocino Transform, internal deformation must occur near the MTJ. Owing to this ~85 km offset between the eastern extension of the SAF (the Bartlett Springs fault) and the Cascadia subduction margin, the Pacific plate converges with the North American plate at the MTJ. The sum of these two motions produces ~N23°E convergence at a rate of ~50 mm/year. Focal mechanisms of earthquakes within this section of the North American crust indicate a compressive stress direction of N20°E (Smith et al. 1993), consistent with the composite convergence direction and measured fault contraction, but ~20°–25° more northerly than the Gorda-North American relative convergence direction alone (Riddihough 1984). Because 10 mm/year of convergence is accommodated by permanent deformation on crustal faults, ~40 mm/year remain to be consumed on the southernmost segment of the Cascadia megathrust, within the GDZ, and by shortening in the MTJ regions. This skewed fault pattern persists for approximately 50 km north of the MTJ, north of which crustal fault orientations parallel the Cascadia subduction zone and the stress field is assumed to be dominated by northeast Gorda-North American convergence alone.

Gulick et al. (2001) interpreted the contrasting northeast- versus northwest-oriented structural fabrics of the subducting Gorda and overlying North American plates, respectively, to indicate a decoupled plate interface (a weak Cascadia megathrust). Both the strength and the seismic potential of the Cascadia subduction zone have been actively discussed in the literature. Although there is evidence for past large earthquake ruptures of the southern Cascadia margin (Clarke & Carver 1992), this subduction zone lacks the seismically well-defined Wadatti-Benioff zone to depths of 200–300 km and the frequent shallow thrust events characteristic of other subduction zones. Riddiough (1984) examined seafloor magnetic anomalies on the Gorda plate and concluded that Gorda-North American plate velocities

have been slowing for the past 12 million years, and since approximately 3 Ma, the southern portion of the Gorda plate has ceased to subduct and is moving parallel to the trench. Nevertheless, on April 25, 1992, an $M_s = 7.1$ underthrusting earthquake (Figure 7) ruptured the southernmost region of the Cascadia subduction zone, ending speculation about the seismic potential of this plate boundary. This event was significant in that it was the first large ($M > 6$) thrust event to occur along the entire Cascadia margin in historic times. Schwartz & Hubert (1997) determined focal mechanisms for tens of the larger aftershocks of this event and inverted them to obtain the regional stress orientations and relative magnitudes. Similar to the general seismicity patterns in the region, the majority of the aftershocks had vertical strike-slip nodal planes and located within the Gorda plate or on the MT at depths between 23–35 km. Shallower events occurred within both the Gorda and North American plates and displayed a large variation in focal mechanisms. Not one of the aftershocks was consistent with northeast underthrusting of the Gorda plate beneath North America seen in the main ($M_s = 7.1$) event. A single stress field characterized by north-northwest, horizontal maximum principal compressive stress was consistent with this diverse set of earthquake geometries. Although this stress direction is nearly perpendicular to convergence between the North American and Gorda plates, it is consistent with the north-south compression in the GDZ northwest of the MTJ. Evidence for failure along the southernmost section of the Cascadia subduction zone comes from the occurrence of the 1992 Cape Mendocino underthrusting earthquake and from measurements of Holocene surface uplift consistent with the 1992 coseismic uplift pattern (Clarke & Carver 1992). Rupture of the Cascadia subduction zone under this stress regime requires that the southernmost region of the Gorda–North American plate boundary is weak.

THE SAN ANDREAS FAULT SYSTEM In northern California, near the MTJ, the SAFS accommodates approximately 40 mm/year transform motion between the Pacific and North American plates (Freymueller et al. 1999). This motion is distributed over a width of ~100 km (Figure 7) between several subparallel strike-slip faults, which are from west to east, the San Andreas (SAF, ~17 mm/year), the Maacama (MF, ~14 mm/year), and the Bartlett Springs (BSF, ~8 mm/year) faults. Development of the SAFS is intricately tied to thermal and mechanical processes occurring within the North American and Pacific lithospheres that accompany MTJ migration. Hot mantle material replacing the Gorda slab heats the crust above the region of upwelling and transform deformation develops simultaneously with thermal re-equilibration of the lithosphere. Furlong et al. (1989) proposed that this process results in thermally induced weakening of the lower crust east of the main SAF that propagates through the upper crust and allows some North American–Pacific plate motion to be accommodated on structures farther east. Castillo & Ellsworth (1993) noted that the eastern strike-slip faults (MF and BSF) are parallel to active northwest striking thrust faults in the forearc of the Cascadia subduction zone, suggesting that the thrust faults persist as zones of weakness and are reactivated to accommodate transform motion south of the MTJ. Northeastern dips of ~60°–70°

apparent in cross-sections of seismicity and oblique strike-slip focal mechanisms (Castillo & Ellsworth 1993) support this interpretation.

Castillo & Ellsworth (1993) performed a thorough analysis of relocated seismicity within the northern SAFS. However, since their study included seismic events that occurred only between 1980 and 1991, we updated the seismicity to include all events in the northern California catalog (Northern California Earthquake Data Center) between 1969 and June 2003 and re-evaluated Castillo & Ellsworth's (1993) primary conclusions. Figure 7 displays this seismicity in both map and cross sectional views and confirms the following major features described by Castillo and Ellsworth: 1) a clear termination of Gorda slab seismicity and a small seismicity gap before activity picks up on the MF and BSF; 2) little seismicity along the SAF; 3) steep northeasterly dip to the MF and BSF; 4) deeper seismicity beneath BSF (15–18 km) than MF (10–12 km); 5) southward shallowing of the base of the MF seismogenic zone between Laytonville and Clear Lake from 10–12 km to 8–10 km; and 6) a decrease in seismicity along the BSF between Round Valley and Lake Pillsbury.

The updated seismicity clearly indicates the southern edge of the Gorda slab (arrows marked in cross-sections and solid black line on map of Figure 7) and shows its location much farther north than previously inferred (dashed line on map of Figure 7) from gravity modeling (Jachens & Griscom 1983). The seismicity indicates a southeastward dip to the southern edge of the Gorda slab as evidenced by its southern dip and more southerly location on the eastern cross-section (Figure 7). Based on seismic tomography, Verdonk & Zandt (1994) located the southern edge of the Gorda slab in the location indicated on Figure 7. Transform motion along the SAFS appears to initiate 25–35 km southeast of Gorda plate termination (Figure 7), consistent also with the results shown in Figure 5. A clear gap in seismicity exists in this region, with the exception of a cluster of rather deep events (15–30 km deep and labeled as the Garberville Swarm in cross-section A-A′ of Figure 7). This pocket of seismicity is clearly separated from the Gorda slab seismicity and not associated with it. Its origin is presently not well understood.

Strike-slip faults accommodating North American–Pacific motion develop within lithosphere that has been thermally weakened by upwelling asthenospheric material replacing the Gorda slab beneath North America. The pattern of the thermal perturbation introduced by asthenospheric upwelling will depend on the specific geometry of the slab window and thus on North American crustal structure. The pattern of high heat flow around the latitude of Clear Lake may be responsible for the shallowing of the MF seismogenic zone from Laytonville to Clear Lake (cross-section A-A′ of Figure 7). The transition from frictional stick-slip behavior (earthquake generation) to stable sliding (no earthquakes) has been shown to be strongly controlled by temperature, with the transition occurring typically between 300°–400° in continental crust. However, an equally plausible explanation for this seismicity shallowing is that lithologic variations created by deformation and metamorphism associated with thickening of the North American crust result in a seismogenic boundary that is deeper in thicker crust. Guzofski & Furlong (2000) approximated the P-T-t (pressure-temperature-time) history and associated

petrologic variations of the North American crust (Franciscan Formation) as it undergoes ephemeral thickening and subsequent thinning associated with passage of the MTJ. They found that as crustal thinning occurs in conjunction with basaltic underplating, a distinct boundary between mid-crustal greenschist and amphibolite facies rocks develops. Experimental data suggest that amphibolite facies rocks are much stronger than greenschist facies rocks (Rutter & Brodie 1992) causing brittle (seismic) deformation to terminate at the greenschist/amphibolite facies boundary. The shallowing of this compositional contact is predicted between Laytonville and Clear Lake and may be the cause of the shallowing seismicity along this profile.

The deeper seismicity of the BSF compared with the MF (Figure 7) may have either a thermal or a compositional origin. Although the eastern fault system (BSF) overlies higher lithospheric temperatures than the western system (MF and SAF), it is possible that a thickened North American crust to the east acts as insulation, ultimately producing lower upper crustal temperatures and a deeper seismogenic zone. Alternatively, west to east compositional variations or crustal thickening that would depress the greenschist to amphibolite or other equivalent metamorphic facies transitions might be responsible for deepening the base of the seismogenic zone beneath the BSF compared with the MF. Finally, the low level of seismicity on the BSF between Round Valley and Lake Pillsbury (Figure 7), as well as the lack of a geomorphically discernable fault trace north of $\sim 39^{\circ}$N, are expected consequences of the deformation resulting from the ephemeral thickening and thinning of the North American crust in response to MTJ passage (crustal conveyor model).

GEODYNAMIC MODEL OF TRIPLE JUNCTION MIGRATION

The Mendocino Crustal Conveyor Model

The concept of a slab window, generated in the wake of the MTJ, had become by the beginning of the 1990s a standard tool in investigations of the tectonic and geologic evolution of the North American plate boundary through California. However, in the late 1990s, new observations of crustal structure in the vicinity of the triple junction required that a rethinking of the crustal and lithospheric scale processes that act at the triple junction be made. In particular, the imaging of substantially thickened crust just to the south of the southern edge of the subducted Gorda slab (Figure 5), i.e., in the wake of the MTJ (Verdonck & Zandt 1994; Beaudoin et al. 1996, 1998; Villasenor et al. 1998), was inconsistent with the crustal thicknesses needed to explain the spatial pattern of the surface heat flow observations. In addition, if the passage of the triple junction were responsible for producing the observed pattern of crustal thickness, then mechanisms associated with MTJ migration that could deform the crust were needed. Up until this point, virtually all models of MTJ tectonics assumed that the overlying North American crust was a relatively passive component of the system.

One first-order consequence of slab removal is that as the slab window is created, the space in the North American lithosphere is partially filled with upwelling asthenospheric material. Furlong & Govers (1999) developed a numerical test of a model in which viscous coupling between the northerly migrating slab and the base of the North American crust drives the deformation in the overlying crust (Figure 8). This occurs as a result of the chilling (stiffening) effects of emplacing viscous mantle adjacent to the slab and beneath the relatively cool North American crust. Their model, the Mendocino Crustal Conveyor (MCC), demonstrated that the crust can be first significantly thickened north of the triple junction and then thinned in a region extending 300 km to the south of the triple junction as a result of processes associated with the opening of the slab window (Figures 8 and 9). As the slab progresses north in concert with the triple junction, this deformational welt will migrate with it, ephemerally thickening and then thinning the North American crust during its passage.

The results of that model predict crustal thickening in advance of the MTJ (North American crustal shortening as material from south of the MTJ is dragged northward) and thinning south of the MTJ (Figure 8*e*). The predicted patterns of crustal thickness that result from this process are in good agreement with the observed patterns of crustal structure (Verdonck & Zandt 1994; Beaudoin et al. 1996, 1998; Villasenor et al. 1998). This active crustal thickening/thinning should perturb the pattern of heat flow and thermal structure, drive surface uplift/subsidence through

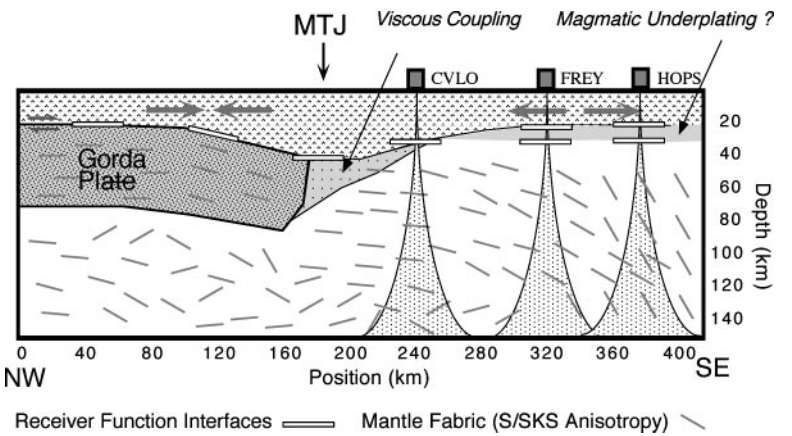

Figure 9 Interpretative view of the processes at the MTJ leading to crustal deformation and mantle flow. Locations of broadband seismic stations, region sampled by seismic data (for teleseismic arrivals; *stippled triangles*), and the inferred location of dominant interfaces that receiver function studies might image are shown. Pattern of crustal thickness and possible mantle fabric that could be imaged by shear wave splitting seismic anisotropy analyses is shown schematically. Inferred extent of regions of viscous coupling and magmatic underplating are shown.

isostatic compensation, and further modify those elevations through any dynamic topography produced by the induced flow in the slab window and mechanical interactions among the plates at the MTJ. All of these effects should migrate with the MTJ, resulting in a crustal pattern that reflects this overprinting of tectonic processes.

Results of the 2-D finite-element MCC numerical model (Furlong & Govers 1999) are shown in Figure 8. Of particular significance to the evolution of the North American crust above the slab window are the rates of crustal thickening and thinning (Figure 8*e*), the patterns of strain within the crust (Figure 8*d*,*f*), patterns of deformation within the slab window, and dynamic forces acting on the base of North America induced by the migration of the slab and flow within the slab window (Figure 8*b*). The model results (Figure 8) are a snapshot of the deformation at 300 kiloyears (model time), but represent a deformational steady state, and thus can be extrapolated forward in time.

Because the model results are an instantaneous picture of deformation associated with triple junction passage, they can be compared with patterns of crustal deformation, such as seismicity and geodetic observations, and, by substituting space for time, we can compare them with the geologic record of deformation south of the triple junction. These instantaneous snapshots can also be migrated in space and integrated in time to simulate the integrated effects of triple junction migration. This produces a model for the Coast Range crust that can be compared to the observed pattern of crustal structure. Patterns of instantaneous deformation (Figure 8) compare well with observations of deformation and structure in the region. Crustal thickening occurs in advance of the MTJ in the region above the decoupled Gorda plate, driven by the northward displacement of crust from south of the triple junction. In the region extending ~50–75 km south from the southern edge of the Gorda plate, predicted crustal deformation rates are low—compatible with the observed low-seismicity zone south of the edge of the subducted slab (Figure 7; Castillo & Ellsworth 1993). Crustal thinning is predicted to occur south of that aseismic region, coincident with the observed seismicity pattern (Castillo & Ellsworth 1993, Miller & Furlong 1988).

Discussion and Implications

The MCC model provides a framework for analyses of the development of the crust in the Coast Ranges, the nature of mantle flow within the slab window, and patterns of deformation as the triple junction migrates. An interpretive model of these crustal and upper mantle consequences of MCC tectonics is shown in Figure 9.

MCC AND COAST RANGE HEAT FLOW Heat flow data from the northern Coast Ranges served to motivate the development of the MTJ slab window model, and now places constraints on the consequences of the MCC. The observed variation in crustal thickness precludes existing thermal models as viable explanations for the heat flow anomaly (Figure 4) and requires a rethinking of the thermal structure

of the Coast Range crust. Previous models of crustal thermal evolution (e.g., Liu & Furlong 1992, Goes et al. 1997) assumed constant crustal thickness and a relatively high temperature for the mantle material emplaced into the MTJ slab window. With the observed thicker crust in the triple junction region, the time it would take for the slab window thermal effects to be seen in surface heat flow is substantially lengthened, inconsistent with observations. MCC crustal deformation produces an initial decrease in surface heat flow (during the period of crustal thickening), followed by a rapid rise in surface heat flow as the crust thins after MTJ passage. This implies that the high heat flow observed in the northern California Coast Ranges is generated by a combination of the effects of crustal thinning (advection) and heat from the emplaced slab window (conduction). Our heat flow modeling indicates that the effects of crustal conveyor crustal thinning satisfy the heat flow observations with a significantly lower temperature for the emplaced mantle (Figure 4; Guzofski & Furlong 2002).

As a result, the pressure-temperature history and resulting metamorphic state of middle crustal rocks will be substantially different from what we previously predicted with a static crustal thickness model (Liu & Furlong 1992). This will affect the rheologic properties of the middle crust. Because MTJ processes are largely responsible for the transformation of accretionary wedge material of the Cascadia margin into the crust of coastal California (including the Franciscan), an improved understanding of the P-T-t history of these rocks should help with understanding the mechanical behavior of the crust throughout California. These modeling results imply that heat flow should reach a minimum in the vicinity of the triple junction. Although direct observations are not available to verify this prediction, it is consistent with the observed heat flow further north along the Cascadia margin (Guzofski & Furlong 2002).

The combination of slab window processes (asthenosphere emplacement and underplating) with the effects of crustal thinning produce the observed patterns of heat flow after the triple junction passage. The thickening and thinning rates for which the thermal model best fits heat flow observations correspond to the deformation rates predicted by the thermal-mechanical modeling of Furlong & Govers (1999) and are consistent with observations of crustal structure. The crustal thinning south of the MTJ is also consistent with the shallowing of SAFS seismicity, south of the Gorda slab edge (Figure 7).

MCC AND MAGMATISM The location of a proposed lower-crustal melt zone near Lake Pillsbury, approximately at the latitude of the FREY seismic station (Figures 1, 5, 9; Beaudoin et al. 1996, Levander et al. 1998), is coincident with the region of predicted maximum crustal thinning (Figure 8). Although more than 100 km south of the southern edge of the Gorda slab, this is also the site of significant upward flow of mantle material into the slab window. This juxtaposition of extensional strain, a >10 km decrease in crustal thickness, and upwelling flow of mantle material all may combine to form and emplace such a melt zone by the combination of pressure-release melting (crustal thinning) and development of a lower-crustal

plumbing system (extensional strain). This may have led to the development of the discrete volcanic centers that occur within the Coast Ranges. If such localization also applies to magmatic underplating of the North American crust, a complex pattern of lower crustal structure and composition would be produced.

The lower temperatures inferred from both the heat flow studies (Guzofski & Furlong 2002) and geochemistry of the Coast Range volcanics and the mantle-wedge affinity for those volcanics all point to a pattern of flow into the slab window from the east. This flow would likely follow a path along the region vacated by the slab as it migrates, and thus we would expect it to be manifest as a mantle flow dipping to the east. Hartog & Schwartz (2000) found that the mantle anisotropy as recorded by shear wave splitting at station HOPS (Figure 1) indicated such a dipping fabric in the upper mantle consistent with this expectation. Additionally, in the upper mantle tomographic study of Benz et al. (1992) an observed high P-wave velocity dipping layer in the vacated slab region (east of the slab window) was problematic. Flow along that path (consistent with the shear wave splitting results) can produce the velocity anomaly seen in the tomography.

MCC AND COAST RANGE TOPOGRAPHY The crustal structure predicted by the MCC model should produce an elevation pattern driven largely by isostatic processes. Embedded in the elevation pattern will also be the effect of dynamic topography generated by the MCC (Figure 8*b*). The combination will produce a pattern of uplift that will migrate with the MTJ that results in a complex two-hump topographic pattern and spatially and temporally varying rates of uplift/subsidence (Furlong et al. 2003). The MCC-predicted dynamic topography can account for the residual isostatic gravity anomaly in the northern Coast Ranges determined by Jachens & Griscom (1983), reproducing the amplitude, wavelength, and location of the ∼40 mgal anomaly. Thus, the primary evidence (isostatic gravity) for the previous estimates of a more southerly trend to the southern edge of the Gorda slab appears to be principally a consequence of dynamic processes in the slab window, rather than the density contrast at the slab edge. This dynamic topography component to the Coast Range topographic evolution is also an important player in the response of the river systems to MTJ migration (Lock & Furlong 2002).

The relative importance of dynamic and isostatic topography has been tested through a comparison of actual elevations in the Coast Ranges to a predicted elevation pattern—the combination of isostatic elevation [from crustal thickness observed in seismic tomography (Villasenor et al. 1998)] and MCC-predicted dynamic topography. The results support this concept that Coast Range elevations are the combination of isostatic uplift and the shorter wavelength effects of the (flexural) dynamic topography (Lock & Furlong 2002, Furlong et al. 2003; J. Lock, unpublished observations).

The geomorphology in the Coast Ranges provide evidence that the drainage pattern in northern California is a reflection of MCC uplift and subsidence (Figures 1, 6). Rivers throughout the Coast Ranges show a pattern of streams generally aligned in a NW-SE direction (∼ the PAC/NOAM relative plate-motion direction),

with a complex pattern of drainage divides, fish-hooked streams, wind gaps, and north- and south-flowing streams superposed. In particular, the location of the present primary drainage divides (Figure 1) coincides with the positions of the two humps in the elevation pattern produced by the interaction of isostatic and dynamic topography (Figure 8). There is evidence in the character of the divides (such as wind gaps and other low-relief features) that these divides migrate with the triple junction—as expected with the crustal thickening and mantle flow of the MCC driving the pattern of Coast Range elevations (Lock & Furlong 2002).

MCC AND COAST RANGE STRAIN Observations of strain in the Coast Ranges of northern California (Prescott & Yu 1986, Lisowski et al. 1991, Freymueller et al. 1999) show a pattern of deformation generally compatible with the shear deformation of the SAFS. The observed strain, however, includes the signal of two types of ongoing deformation: (*a*) interseismic elastic strain released periodically in earthquakes on the Cascadia subduction interface and the other major faults in the region and (*b*) bulk strain associated with crustal conveyor shortening and extension. Freymueller et al. (1999) assumed that virtually all of the observed deformation south of the MTJ was fault-related interseismic strain, and, with that assumption, partitioned the observed strains onto deep slip associated with each of the major fault systems in the region (San Andreas, Maacama, and Bartlett Springs). They noted that their inferred fault displacements differed from the fault displacements observed (both geologically and geodetically) along the southern extensions of the same faults (e.g., Lisowski et al. 1991). Although these differences may reflect a spatial and temporal variability along the plate boundary fault zones, the observed pattern of crustal thickness and the crustal thinning that occurs south of the MTJ argue that some part of the strain field observed with GPS measurements is associated with the bulk strain producing the crustal thinning, which will vary significantly spatially. In Figure 8*f*, the observed strain rate in the orientation of the MCC model profile is compared to model predictions (Furlong & Guzofski 2000, Furlong et al. 2003). The observed rate was obtained by differencing the GPS results from Freymueller et al. (1999). There is a good match in both sign and amplitude for the model predicted and observed strain rates.

The spatial pattern of crustal conveyor strain is an important component of any interpretation of crustal deformation observations along the northern SAF. This strain does not contribute to strike-slip faulting (and neither does strike-slip faulting significantly contribute to the bulk crustal thinning); thus, evaluations of seismic potential along any of the major faults north of the San Francisco Bay (the region affected by crustal conveyor deformation) using observed strain patterns to explain interseismic fault loading must account for this component. The strain accumulation rate for some faults is reduced by considering these effects, whereas other fault segments have a higher strain accumulation rate than would be apparent from an analysis of the observations without consideration of crustal conveyor effects.

As previously noted in the seismicity section of this review, the lack of a discernable geomorphic manifestation of the SAF north of approximately 39°N is an

expected consequence of the interplay between San Andreas shear deformation and crustal conveyor bulk deformation. In that region, the North American crust is predicted to be moving at essentially the same velocity as the Pacific plate, and, thus, although there is a fundamental boundary separating Pacific and North American crust, there may be little relative motion between them.

North of the triple junction, the Gorda slab subducts beneath North America with a northeasterly relative motion. This drives interseismic northeasterly shortening in the overlying North American crust north of the triple junction, which will combine with the northwesterly directed MCC shortening, producing, on short interseismic timescales, an apparent northerly directed shortening just to the north of the triple junction. Moving north, a decrease in rates of MCC crustal shortening combined with Cascadia-related seismic-cycle shortening would lead to an apparent rotation in the observed (GPS) crustal deformation into the Gorda–North American relative motion direction. However, on geologic timescales, MCC shortening should dominate. This may explain the pattern of faulting and fault deformation identified by McCrory (2000) for the accretionary margin region north of the MTJ.

CONCLUSION

With the passage of the MTJ, profound and fundamental changes in the evolution of the western margin of North American lithosphere occur. As a result of a superb database of observations, with a more than a three-decade history of detailed studies, an understanding of the consequences of triple junction migration is unfolding. Of particular importance in extending this understanding to other plate boundary regimes is the realization that substantial and complex interactions can occur among the plates below the surface. The notion of large amounts of crustal deformation being driven by viscous coupling within the slab window is unnerving but also exciting. The potential importance of such lower-crustal upper mantle viscous coupling is of some concern because the record of this activity is not necessarily obvious in near-surface faulting or other aspects of the geologic record—so it could be a hidden process and difficult to identify. Yet it appears to play the dominant role in converting accretionary margin materials into continent-like crust. From the work that has been done along the SAFS in response to MTJ passage, we can begin to identify the signature of this style of tectonism and apply that knowledge elsewhere. Although the FFT type of triple junction represented by the MTJ is not overly common, triple junctions that generate slab windows (particularly those involving a ridge) have occurred numerous times in geologic history. In all of these cases, significant modifications to the overlying crust are likely.

Additionally, the San Andreas plate boundary system of faults resides primarily in the crust modified by the MCC. Thus, as we work to improve our understanding of the nature of faulting, processes of rupture initiation and propagation, and the underlying cause of asperities and other fault-locking behavior, we need to understand the evolution of that crust. The depth distribution of seismicity, the

patterns of fault creep, and the fundamental question of the strength of the SAF are all likely related to the consequences of the migration of the MTJ.

ACKNOWLEDGMENTS

Many of the ideas presented here are the result of far-ranging discussions with graduate students in the Geodynamic Research Group at Penn State, including Chris Guzofski, Jaime Whitlock, Jane Lock, Gavin Hayes, and Rocco Malservisi, students at UC Santa Cruz, including Renate Hartog, Mike Hagerty, and Curtis Hall, and Harvey Kelsey at Humbolt State University. Additionally, continued collaborations with Rob Govers at Utrecht University have helped with numerical modeling. Financial support has been provided to KPF and colleagues for this research under NSF grants EAR-99,02937 and EAR-02,21133.

LITERATURE CITED

Atwater T. 1970. Implications for plate tectonics for the Cenozoic tectonic evolution of western North America. *Geol. Soc. Am. Bull.* 81:3513–35

Atwater T, Stock J. 1998. Pacific-North America plate tectonics of the Neogene Southwestern United States—an update. *Int. Geol. Rev.* 40:375–402

Barr SR, Temperley S, Tarney J. 1999. Lateral growth of the continental crust through deep level subduction-accretion: a re-evaluation of central Greek Rhodope. *Lithos* 46:69–94

Beaudoin BC, Godfrey NJ, Klemperer SL, Lendl C, Trehu AM, et al. 1996. Transition from slab to slabless: results from the 1993 Mendocino triple junction seismic experiment. *Geology* 24:195–99

Beaudoin BC, Hole JE, Klemperer C, Trehu AM. 1998. Location of the southern edge of the Gorda slab and evidence for an adjacent asthenospheric window; results from seismic profiling and gravity. *J. Geophys. Res.* 103:30101–15

Beaudoin BC, Magee M, Benz H. 1994. Crustal velocity structure north of the Mendocino triple junction. *Geophys. Res. Lett.* 21:2319–22

Benz HM, Zandt G, Oppenheimer DH. 1992. Lithospheric structure of northern California from teleseismic images of the upper mantle. *J. Geophys. Res.* 97:4791–807

Blake MC, Jayko AS, McLaughlin RJ. 1985. Tectonostratigraphic terranes of the northern Coast Ranges, California. In *Tectonostratigraphic Terranes of the Circum-Pacific Region*, ed. DG Howell, pp. 159–86. Houston, TX: Circum-Pac. Counc. Energy Miner. Resour.

Bohannon RG, Parsons T. 1995. Tectonic implication of post-30 Ma Pacific and North American relative plate motions. *Geol. Soc. Am. Bull.* 107:937–59

Castillo DA, Ellsworth WL. 1993. Seismotectonics of the San Andreas fault system between Point Arena and Cape Mendocino in northern California: implication for the development and evolution of a young transform. *J. Geophys. Res.* 98:6543–60

Clarke SH Jr, Carver GA. 1992. Late Holocene tectonics and paleoseismicity, southern Cascadia subduction zone. *Science* 255:188–92

DeMets C, Dixon TH. 1999. New kinematic models for Pacific-North America motion from 3 Ma to present. I. Evidence for steady

motion and biases in the NUVEL-1A model. *Geophys. Res. Lett.* 26:1921–24

Dickinson WR. 1997. Tectonic implications of Cenozoic volcanism in coastal California. *Geol. Soc. Am. Bull.* 109:963–54

Dickinson WR, Snyder WS. 1979. Geometry of subducted slabs related to the San Andreas transform. *J. Geol.* 87:609–27

Dziak RP, Fox CG, Bobbitt AM, Goldfinger C. 2001. Bathymetric map of the Gorda plate: structural and geomorphological processes inferred from multibeam surveys. *Mar. Geophys. Res.* 22:235–50

Eaton JP. 1981. Distribution of aftershocks of the November 8, 1980, Eureka, California earthquake. *Earthq. Notes.* 52:44–45

Ernst WG. 1970. Tectonic contact between the Franciscan mélange and the Great Valley sequence, crustal expression of a late Mesozoic benioff zone. *J. Geophys. Res.* 75:886–902

Fox KF, Fleck RJ, Curtis GH, Meyer CE. 1985. Implications of the northwestwardly younger age of the volcanic rocks of west-central California. *Geol. Soc. Am. Bull.* 96:647–54

Freymueller JT, Murray MH, Segall P, Castillo D. 1999. Kinematics of the Pacific North America plate boundary zone, northern California. *J. Geophys. Res.* 104:7419–41

Furlong KP. 1984. Lithospheric behavior with triple junction migration, an example based on the Mendocino triple junction. *Phys. Earth Planet. Int.* 36:213–23

Furlong KP, Govers R. 1999. Ephemeral crustal thickening at a triple junction: the Mendocino crustal conveyor. *Geology* 27:127–30

Furlong KP, Guzofski C. 2000. Thermal rheological evolution of the Franciscan crust: implications for earthquake processes. *Proc. 3rd Conf. Tecton. Probl. San Andreas Fault Syst.*, ed. G Bokelmann, RL Kovach, pp. 112–27. Stanford, CA: Stanford Univ. Press

Furlong KP, Hugo WD, Zandt G. 1989. Geometry and evolution of the San Andreas Fault Zone in northern California. *J. Geophys. Res.* 94:3100–10

Furlong KP, Lock J, Guzofski C, Whitlock J, Benz H. 2003. The Mendocino crustal conveyor: making and breaking the California crust. *Int. Geol. Rev.* 45(9):767–79

Goes S, Govers R, Schwartz SY, Furlong KP. 1997. Three-dimensional thermal modeling for the Mendocino triple junction area. *Earth Planet. Sci. Lett.* 148:45–57

Guzofski CA, Furlong KP. 2002. Migration of the Mendocino triple junction and ephemeral crustal deformation: Implications for California Coast Range heat flow. *Geophys. Res. Lett.* 29:12-1–4

Hall CE, Schwartz SY, Sampson DE, Furlong KP. 2001. Crustal structure near the Mendocino Triple Junction, California from broadband receiver functions. *EOS Trans. Am. Geophys. Union* 82:F1113 (Abstr.)

Hartog R, Schwartz SY. 2000. Subduction-induced strain in the upper mantle east of the Mendocino triple junction, California . *J. Geophys. Res.* 105:7909–30

Hayes GP, Furlong KP, Ammon C, Hall C. 2003. Crustal structure evolution in response to the passage of the Mendocino triple junction: a receiver function analysis. *Eur. Geophys. Soc.* 5:4626 (Abstr.)

Henstock TJ, Levander A, Hole JA. 1997. Deformation in the lower crust of the San Andreas fault system in Northern California. *Science* 278:650–53

Holbrook WS, Lizarralde D, McGeary S, Bangs N, Diebold J. 1999. Structure and composition of the Aleutian Island arc and implications for continental crustal growth. *Geology* 27:31–34

Hole JA, Beaudoin BC, Henstock TJ. 1998. Wide-angle seismic constraints on the evolution of the deep San Andreas plate boundary by Mendocino triple junction migration. *Tectonics* 17:802–18

Hole JA, Beaudoin, BC, Klemperer SL. 2000. Vertical extent of the newborn San Andreas fault at the Mendocino triple junction. *Geology* 28:1111–14

Jachens RC, Griscom A. 1983. Three-dimensional geometry of the Gorda plate beneath northern California. *J. Geophys. Res.* 88:9375–92

Johnson LE, Fryer P, Taylor B, Silk M, Jones

DL, et al. 1991. New evidence for crustal accretion in the outer Mariana fore arc: cretaceous radiolarian cherts and mid-ocean ridge basalt-like lavas. *Geology* 19:811–14

Johnson CM, O'Neil JR. 1984. Triple junction magmatism: a geochemical study of Neogene volcanic rocks in western California. *Earth Planet. Sci. Lett.* 71:241–62

Kelsey HM, Carver GA. 1988. Late Neogene and Quarternary tectonics associated with northward growth of the San Andreas transform fault, northern California. *J. Geophys. Res.* 93:4797–819

Kimura G, Ludden JN, Desrochers JP, Hori R. 1993. A model of ocean-crust accretion for the Superior province, Canada. *Lithos* 30:337–55

Lachenbruch AH, Sass JH. 1980. Heat flow and energetics of the San Andreas fault zone. *J. Geophys. Res.* 85:6185–222

Lay T, Given J, Kanamori H. 1982. Long-period mechanism of the 8 November 1980 Eureka, California, earthquake. *Bull. Seismol. Soc. Am.* 72:439–56

Levander A, Henstock TJ, Meltzer AS, Beaudoin BC, Trehu AM, Klemperer SL. 1998. Fluids in the lower crust following Mendocino triple junction migration: active basaltic intrusion? *Geology* 26:171–74

Lisowski M, Savage JC, Prescott WH. 1991. The velocity field along the San Andreas Fault in central and southern California. *J. Geophys. Res.* 96:8369–89

Liu M, Furlong KP. 1992. Cenozoic volcanism in California Coast Ranges: numerical solutions. *J. Geophys. Res.* 97:4941–51

Liu M, Zandt G. 1996. Convective thermal instabilities in the wake of the migrating Mendocino triple junction, California. *Geophys. Res. Lett.* 23:1573–76

Lock J, Furlong KP. 2002. Geomorphic insights into the links between mantle flow and crustal deformation in the northern California Coast Ranges. *EOS Trans. Am. Geophys. Union* 83:F1341 (Abstr.)

Mason RG, Raff AD. 1961. A magnetic surfey off the west coast of North America 32 N to 42 N. *Geol. Soc. Am. Bull.* 72:1259–65

McCaffrey R, Long MD, Goldfinger C, Zwick PC, Nabelek JL, et al. 2000. Rotation and plate locking at the southern Cascadia subduction zone. *Geophys. Res. Lett.* 27:3117–20

McCrory PA. 2000. Upper plate contraction north of the migrating Mendocino triple junction, northern California: implications for partitioning of strain. *Tectonics* 19:1144–60

McLennan SM, Taylor SR. 1982. Geochemical constraints on the growth of the continental crust. *J. Geology.* 90:347–61

Miller CK, Furlong KP. 1988. Thermal-mechanical controls on seismicity depth distributions in the San Andreas fault zone. *Geophys. Res. Lett.* 15:1429–32

Murray MH, Marshall GA, Lisowski M, Stein RS. 1996. The 1992 M = 7 Cape Mendocino, California earthquake: coseismic deformation at the south end of the Cascadia megathrust. *J. Geophys. Res.* 101:17707–25

Page BM, Brocher TM. 1993. Thrusting of the central California margin over the edge of the Pacific plate during the transform regime. *Geology* 21:635–38

Prescott WH, Yu SB. 1986. Geodetic measurement of horizontal deformation in the northern San Francisco bay region, California. *J. Geophys. Res.* 91:7475–84

Riddihough RP. 1984. Recent movements of the Juan de Fuca plate system. *J. Geophys. Res.* 89:6980–94

Rudnick RL, Fountain DM. 1995. Nature and composition of the continental crust: a lower crustal perspective. *Rev. Geophys.* 33:267–309

Rutter EH, Brodie KH. 1992. Rheology of the lower crust. In *Continental Lower Crust*, ed. DM Fountain, R Arculus, RW Kay. New York: Elsevier. 213 pp.

Schwartz SY, Hubert A. 1997. The state of stress near the Mendocino triple junction from inversion of earthquake focal mechanisms. *Geophys. Res. Lett.* 24:1263–66

Sengor AMC, Natalin BA. 1996. Turkic-type orogeny and its role in the making of the continental crust. *Annu. Rev. Earth Planet. Sci.* 24:263–337

Silver EA. 1971. Tectonics of the Mendocino triple junction. *Geol. Soc. Am. Bull.* 82:2965–78

Simpson RW, Lienkaemper JJ, Galehouse JS. 2001. Variations in creep rate along the Hayward fault, California interpreted as change in depth of creep. *Geophys. Res. Lett.* 28:2269–72

Smith SW, Knapp JS, McPherson RC. 1993. Seismicity of the Gorda plate, structure of the continental margin, and an eastward jump of the Mendocino triple junction. *J. Geophys. Res.* 98:8153–71

Stein M, Goldstein SL. 1996. From plume head to continental lithosphere in the Arabian-Nubian shield. *Nature* 382:773–78

ten Brink US, Shimizu N, Molzer PC. 1999. Plate deformation at depth under Northern California; slap gap or stretched slab? *Tectonics* 18:1084–98

Trehu AM, Mendocino Working Group. 1995. Pulling the rug out from under California: seismic images of the Mendocino triple junction region. *EOS Trans. Am. Geophys. Union* 76(38):369380–81

Velasco AA, Ammoon CJ, Lay T. 1994. Recent large earthquake near Cape Mendocino and in the Gorda plate: broadband source time functions, fault orientations, and rupture complexities. *J. Geophys. Res.* 99:711–28

Verdonck D, Zandt G. 1994. Three-dimensional crustal structure of the Mendocino triple junction region from local earthquake travel times. *J. Geophys. Res.* 99:23843–58

Villasenor A, Benz H, Stanley D. 1998. *Seismic image of the San Andreas fault system using local earthquake data*. Presented at Annu. IRIS Workshop, 10th, Univ. Calif., Santa Cruz

Whitlock JS, Furlong KP, Lesher CE, Furman T. 2001. The Juan de Fuca Slab-window and Coast Range Volcanics, California: correlation between subducted slab age and mantle wedge geochemistry. *EOS Trans. Am. Geophys. Union* 82:F1186 (Abstr.)

Wilson DS. 1989. Deformation of the so-called Gorda plate. *J. Geophys. Res.* 94:3065–75

Zandt G. 1981. Seismic images of the deep structure of the San Andreas fault system, central coast ranges, California. *J. Geophys. Res.* 86:5039–52

Zandt G, Furlong KP. 1982. Evolution and thickness of the lithosphere beneath coastal California. *Geology* 10:376–81

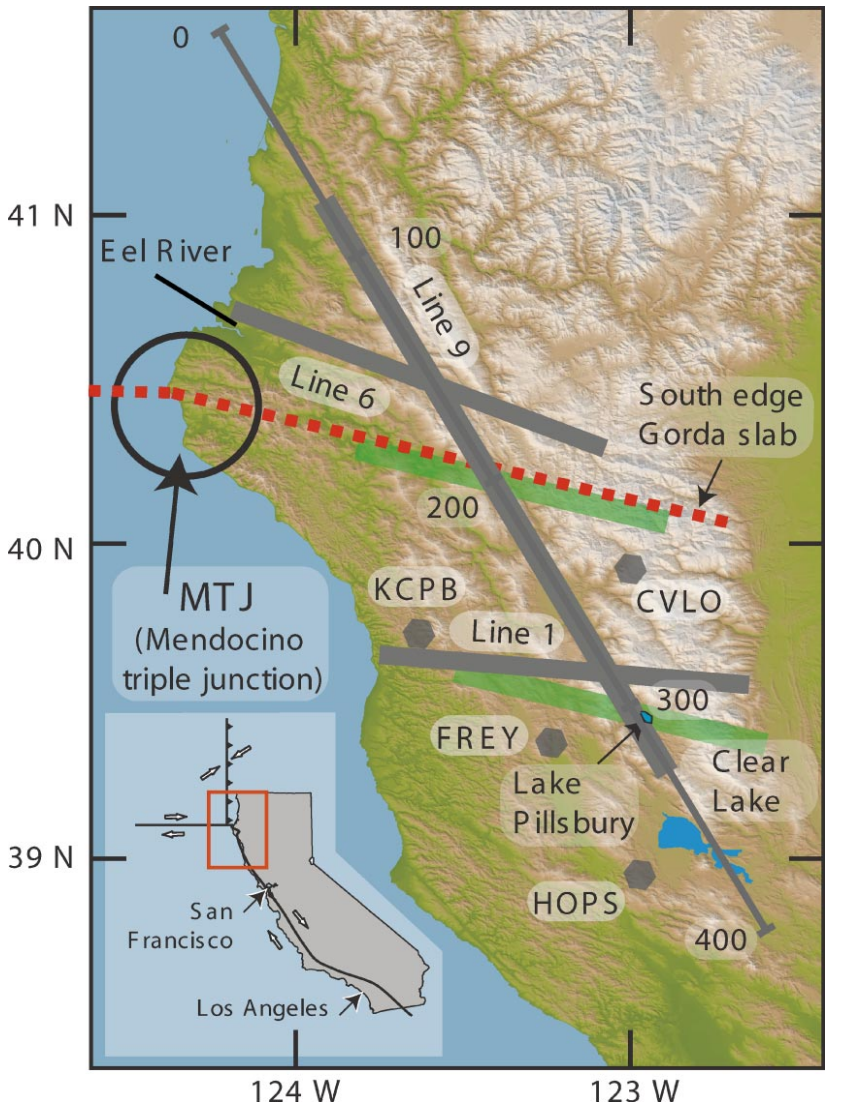

Figure 1 Region of Northern California primarily affected by the recent migration of the Mendocino triple junction. Region of high elevations is the Coast Ranges. Gray lines indicate approximate location of seismic lines (*lines 1*, *6*, and *9*) in the region from the Mendocino triple junction seismic experiment (MTJSE). The locations of four broadband seismic stations (named CVLO, FREY, HOPS, and KCPB) are shown. Numbers along profile correspond to the distances (kilometers) referenced in the numerical modeling, and indicated in Figures 4, 5, 8, and 9. Green bands oriented west-northwest locate the main divides between river systems in the Coast Ranges. The red dashed line shows the preferred location for the southern edge of the Gorda slab. The inset shows the plate tectonic configuration of the region.

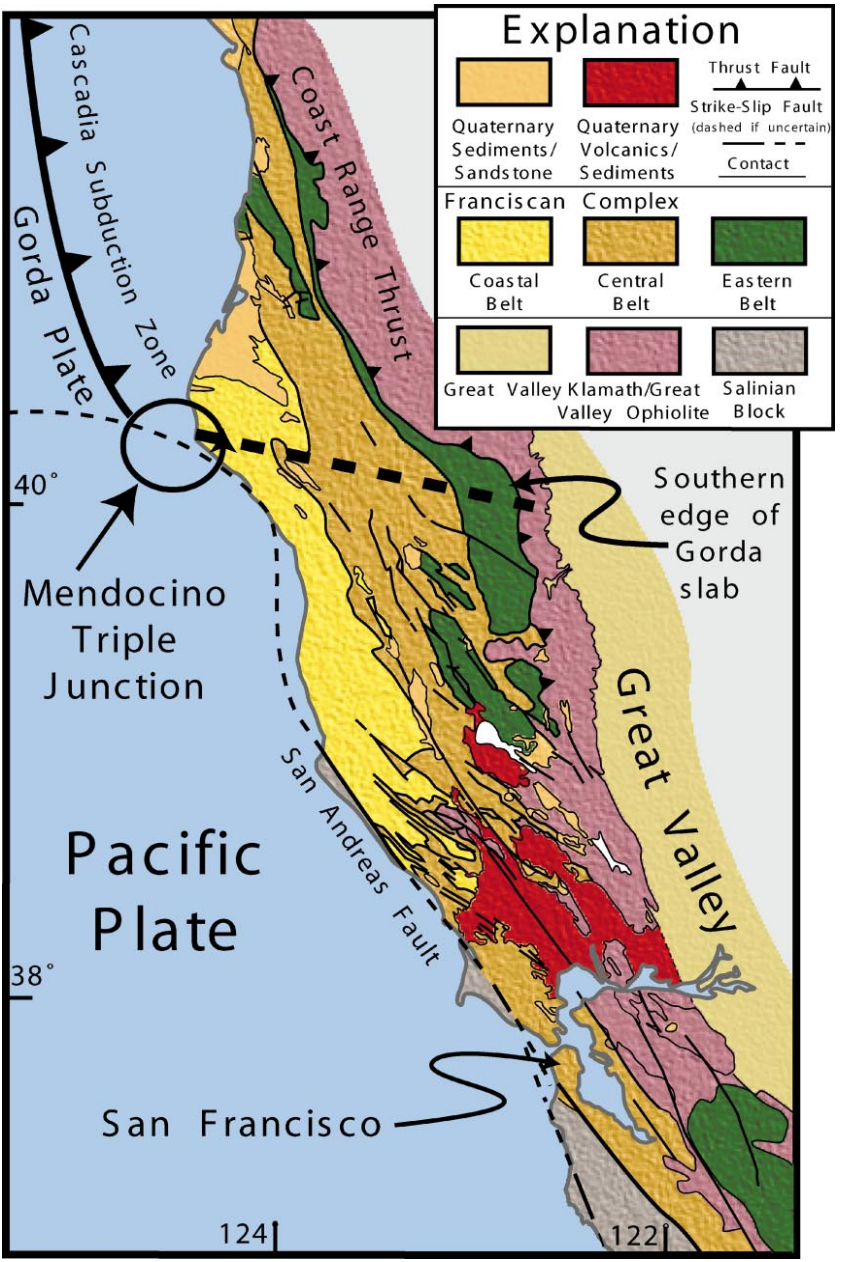

Figure 3 Simplified geologic map of northern coastal California. Young volcanic rocks north of San Francisco Bay locally overlie the three belts of the Franciscan Complex. Primary crustal thickening occurs within the Central belt of the Franciscan Complex between 40°N and 41°N.

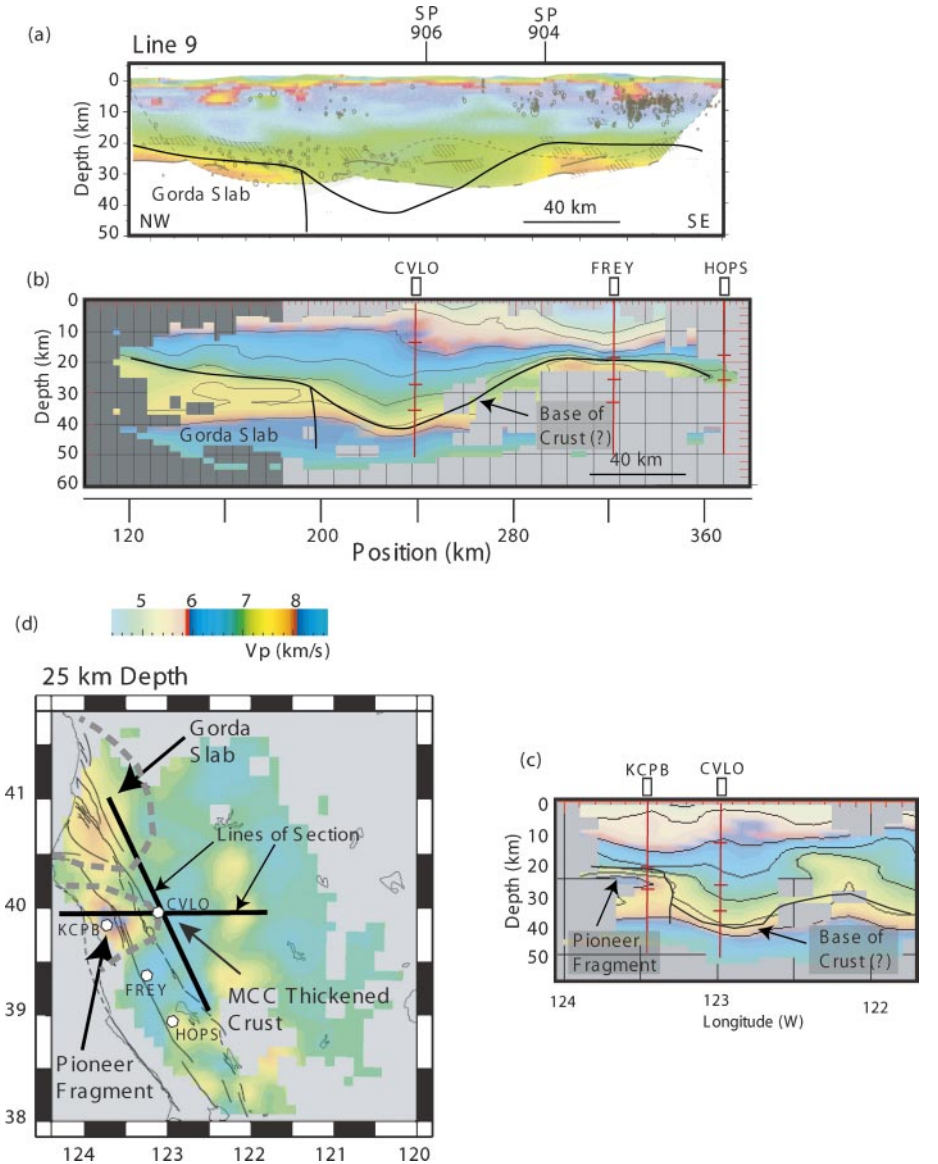

See legend on next page

Figure 5 Seismic images of crust and uppermost mantle in the Coast Ranges of northern California. (*a*) Results from line 9 of the MTJSE (Beaudoin et al. 1996). Our inferred position of the base of the crust is shown, as is the extent of the Gorda slab in the cross-section. Positions of shot points (SP) 906 and 904 are shown. (*b*) Crustal tomography cross-section for profile equivalent to line 9, derived from the seismic tomography results of Villasenor et al. (1998). Base of crust and extent of Gorda slab in cross-section are shown. Comparison of receiver function interfaces (Figure 6) at broadband seismic stations (CVLO, FREY, and HOPS) with tomographic image is shown by red vertical profiles. (*c*) East-west profile in crustal tomography showing base of crust, extent of the Pioneer Fragment. The relationship between receiver function interfaces (Stations KCPB and CVLO) and tomography is shown by red vertical profiles. (*d*) Map view of crustal tomography at 25 km depth. Solid lines indicate extent of profiles in (*a*), (*b*), and (*c*). Dashed gray lines outline the extent of the Gorda slab (at 25 km depth) and the Pioneer Fragment. Locations of broadband seismic stations are labeled.

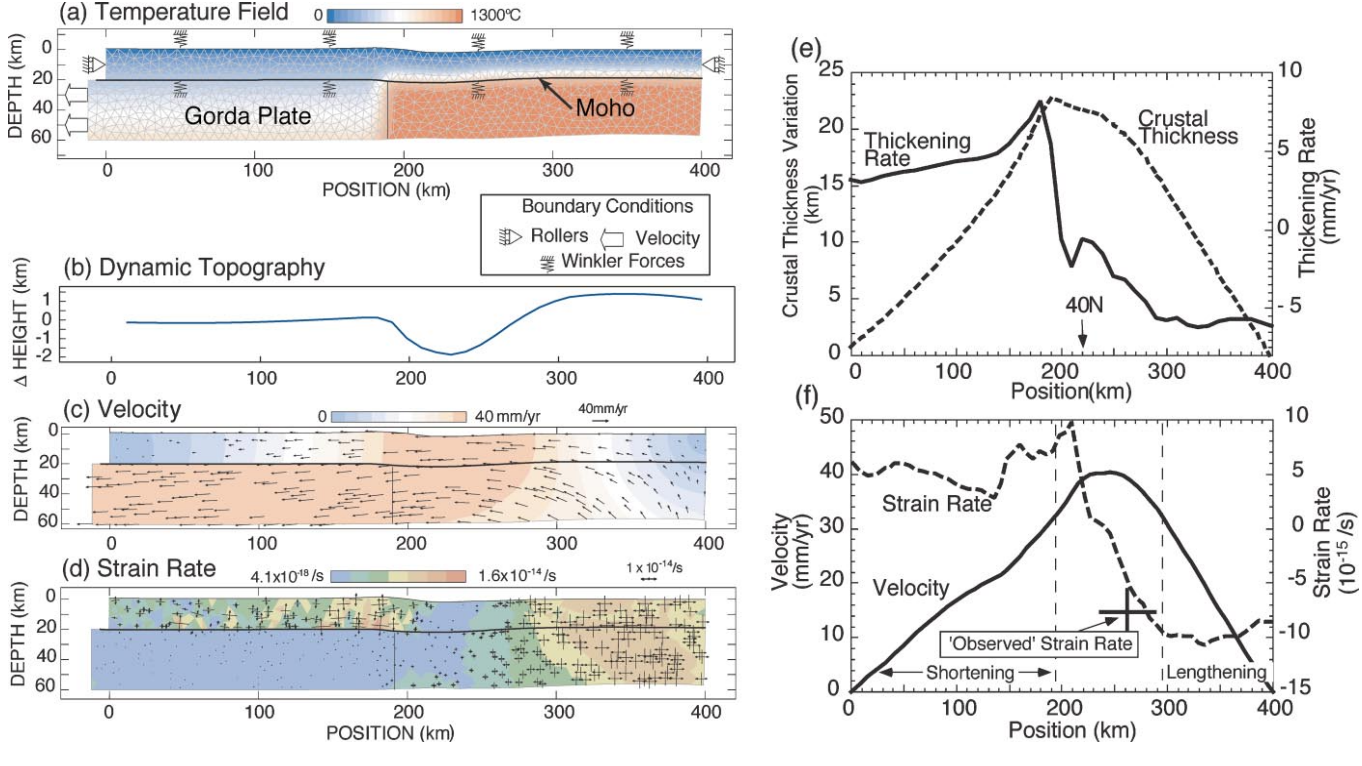

See legend on next page

Figure 8 Results of numerical model testing the Mendocino Crustal Conveyor process (adapted from Furlong & Govers 1999). (*a*) Model configuration, boundary conditions, and temperature structure. (*b*) Results for dynamic topography presented as the change in elevation. This effect will combine with elevations driven by variations in crustal thickness. (*c*) Velocity field (relative to a fixed North America) showing rigid motion of the Gorda slab, patterns of mantle flow in the slab window, and velocities in the crust that lead to shortening and extension. (*d*) Patterns of deformation shown as strain rate. Little deformation occurs in the Gorda slab and in the crust immediately south of the triple junction. Shortening strain occurs north of the triple junction, whereas extension and thinning occurs in the region approximately 100 km south of the triple junction. (*e*) Rate of crustal thickening derived from results shown in panel (*d*), and resulting increase in crustal thickness obtained from integrating the thickening rate curve. (*f*) Strain rate in the near-surface and surficial velocity field along profile. Observed strain rate is obtained from GPS results of Freymueller et al. (1999).

Annual Review of Earth and Planetary Science
Volume 32, 2004

CONTENTS